ELSEVIER

Biophysical Chemistry 116 (2005) 145 – 157

Biophysical Chemistry

http://www.elsevier.com/locate/biophyschem

Regulation of oxidative phosphorylation in intact mammalian heart in vivo

Bernard Korzeniewski[a,b,*], Akinori Noma[a], Satoshi Matsuoka[a]

[a]*Department of Physiology and Biophysics, Kyoto University Graduate School of Medicine, Kyoto, Japan*
[b]*Faculty of Biotechnology, Jagiellonian University, Kraków, Poland*

Received 10 December 2004; received in revised form 12 April 2005; accepted 12 April 2005
Available online 25 April 2005

Abstract

A dynamic computer model of oxidative phosphorylation in intact heart was developed by modifying the model of oxidative phosphorylation in intact skeletal muscle published previously. Next, this model was used for theoretical studies on the regulation of oxidative phosphorylation in intact heart in vivo during transition between different work intensities. It is shown that neither a direct activation of ATP usage alone nor a direct activation of both ATP usage and substrate dehydrogenation, including the calcium-activated tricarboxylate acid cycle dehydrogenases, can account for the constancy of [ADP], [PCr], [P_i] and [NADH] during a significant increase in oxygen consumption and ATP turnover encountered in intact heart in vivo. Only a direct activation of all oxidative phosphorylation complexes in parallel with a stimulation of ATP usage and substrate dehydrogenation enabled to reproduce the experimental data concerning the constancy of metabolite concentrations. The molecular background of the differences between heart and skeletal muscle in the kinetic behaviour of the oxidative phosphorylation system is also discussed.

Keywords: Respiration rate; Oxygen consumption; Parallel activation; Intact heart; Calcium signalling; Computer model

1. Introduction

The blood pumping by the heart constitutes a form of mechanical work and is driven by cyclic contraction of cardiac myocytes. The energy for this contraction comes from the hydrolysis of ATP to ADP and inorganic phosphate (P_i). ATP is utilized by actomyosin-ATPase, sarcoplasmic reticulum Ca^{2+}-ATPase, sarcolemmal Na^+/K^+-ATPase and by basic processes keeping the cell alive. Essentially the only source of ATP in heart is oxidative phosphorylation in mitochondria because no changes in [PCr] take place in intact heart in vivo [1,2]. The rate of respiration and ATP turnover in heart can increase several times during transition from a low beating frequency to a high beating frequency (workload). Therefore, the rate of ATP production by oxidative phosphorylation must be adjusted to the current energy demand in order to match exactly the rate of ATP consumption.

Three main mechanisms of adjusting the rate of ATP supply by oxidative phosphorylation have been proposed in the literature. Due to the first mechanism, which can be called the output-activation mechanism, only the ATP usage block (output of the system) is directly activated by calcium ions (Ca^{2+}) during elevated muscle work, while oxidative phosphorylation is activated only indirectly, through the negative feedback involving an increase in [ADP] (and [P_i]) [3,4]. The input/output activation mechanism involves the direct activation of substrate dehydrogention (input of the system), especially the "key" TCA cycle dehydrogenases: pyruvate dehydrogenase, isocitrate dehydrogenase and 2-oxoglutarate dehydrogenase by Ca^{2+} in parallel with the activation of ATP usage [5,6]. Finally, due to the each-step-activation mechanism or parallel-activation mechanisms some cytosolic factor (e.g. Ca^{2+}) activates directly all oxidative phosphorylation enzymes, substrate dehydrogenation and ATP usage [8–10].

Abbreviations: MCA, Metabolic Control Analysis; VO_2, respiration rate; PCr, phosphocreatine; Cr, creatine.

* Corresponding author. Faculty of Biotechnology, Jagiellonian University, ul. Gronostajowa 7, 30-387 Kraków, Poland. Tel.: +48 12 664 63 73; fax: +48 12 664 69 02.
E-mail address: benio@mol.uj.edu.pl (B. Korzeniewski).

0301-4622/$ - see front matter © 2005 Elsevier B.V. All rights reserved.
doi:10.1016/j.bpc.2005.04.001

The parallel-activation mechanism is able to account for several properties of the oxidative phosphorylation in intact skeletal muscle, including the stability of [ADP], [P_i], PCr/Cr, NADH/NAD^+ and Δp during rest-to-work transition, the much steeper phenomenological VO_2/[ADP] relationship in intact skeletal muscle than in isolated muscle mitochondria, the 2 to 4 times greater maximum oxygen consumption in intact skeletal muscle than in isolated mitochondria, skinned fibres or muscle homogenate [11,12] when scaled for the amount of mitochondrial proteins, the increase in the relative slope of the VO_2/[ADP] relationship as a result of muscle training [13], the greater VO_2 at a given [ADP] and amount of mitochondrial protein in trained muscle than in untrained muscle and in untrained muscle than in hypothyroid muscle [14], the asymmetry of the half-transition time $t_{1/2}$ for [PCr] between the on-transient (rest-to-work transition) and off-transient (work-to-rest transition) [14], the PCr recovery overshoot [14] and the variability of the kinetic properties of oxidative phosphorylation in different muscles and various experimental conditions [14]. Therefore, the idea of the each-step activation in intact skeletal muscle seems to be well founded.

The kinetic properties of the bioenergetic system in heart muscle, which is never at rest under physiological conditions, seem to differ in some important respects from the kinetic properties of this system in skeletal muscle. The mitochondria volume in heart is several times greater than in skeletal muscle. Even more important, a very stable homeostasis of intermediate metabolite concentrations can be observed in intact heart in vivo at different work intensities—[ADP], [PCr] and [P_i] do not change at all [1,2], while changes in mitochondrial [NADH] are very small [15]. On the other hand, the changes of these metabolite concentrations between rest and work in skeletal muscle, although relatively small, are quite significant. There exist some additional minor differences—for example the total creatine pool (PCr+Cr) seems to be smaller in heart than in skeletal muscle. For all these reasons, the conclusions concerning the regulation of oxidative phosphorylation in skeletal muscle may be not fully applicable to intact heart.

The purpose of the present article is to develop a computer dynamic model of oxidative phosphorylation in intact heart in vivo by modifying the previously published model of oxidative phosphorylation in intact skeletal muscle [7,11], and then to use this model for theoretical studies on the regulation of oxidative phosphorylation in intact heart in vivo. Our computer simulations decidedly support the each-step-activation mechanism, showing that probably all oxidative phosphorylation complexes must be directly activated by some factor (e.g. Ca^{2+}) in parallel with the direct activation of ATP usage and substrate dehydrogenation during transition from low work to high work in intact heart. At the same time, we explain the molecular background of the differences between the kinetic properties of oxidative phosphorylation in skeletal muscle and in heart.

2. Theoretical procedures

2.1. Model of oxidative phosphorylation in intact heart

A model of oxidative phosphorylation in intact heart was developed by modifying the previously published model of oxidative phosphorylation in intact skeletal muscle [7,11]. The latter model takes into account explicitly the following enzymes/processes/metabolic blocks: substrate dehydrogenation, complex I, complex III, complex IV (cytochrome *c* oxidase), proton leak, ATP synthase, ATP/ADP carrier, phosphate carrier, adenylate kinase, creatine kinase and ATP usage system. The general scheme of the oxidative phosphorylation system is presented in Fig. 1. The time variations of the metabolite concentrations that constitute independent variables (NADH, ubiquinol, reduced form of cytochrome *c*, O_2, internal protons, internal ATP, internal P_i, external ATP, external ADP, external P_i, external protons, PCr) are expressed in the form of a set of ordinary differential equations. The set of differential equations is integrated numerically using the Gear procedure. The simulation program is written in FORTRAN.

In the present study the model of oxidative phosphorylation in skeletal muscle was modified in order to take into account the specific properties of the bioenergetic system in intact heart muscle. First of all, the relative mitochondria volume (percent of the entire cell volume) was increased from 6.7% to 23%, according to the higher mitochondria content in heart [16]. Consequently, the rate constants for each enzyme/process/block of reactions (substrate dehydrogenation, complex I, complex III, complex IV, proton leak, ATP synthase, ATP/ADP carrier, phosphate carrier) were increased 3.43 (23%/6.7%) times, because the rate constants contain implicitly enzyme concentrations. Secondly, the total creatine pool [PCr]+[Cr] was decreased to 25 mM [17–20] and the total phosphate pool $3[ATP]_e+2[ADP]_e+[AMP]_e+[PCr]_e+[P_i]_e+(3[ATP]_i+2[ADP]_i+[P_i]_i)/R_{cm}$ was decreased to 45.6 mM in order to obtain $[P_i]_e$ equal to about 2.5 mM at low heart work. Here, subscript 'e' means 'cytosolic', subscript 'i' means 'mitochondrial' and $R_{cm}=77\%/23\%=3.35$ is the ratio of cytosol volume to mitochondria volume. This caused that in heart the $[P_i]_e$ was significantly smaller at a given $[ADP]_e$ than in skeletal muscle, what affected the phenomenological VO_2–[ADP] relationship (see Discussion). Lastly, the rate constant of ATP usage at the lowest heart work was assumed to be 17.8 (3.43 * 5.2) times greater than the rate constant of ATP usage in resting skeletal muscle. 3.43 is the scaling factor for the increased mitochondria volume (oxidative phosphorylation activity) as discussed above, while 5.2 was adjusted in order to obtain experimental values of [ADP], [P_i] and PCr/Cr. The concentrations of intermediate metabolites (ADP, ATP, PCr, P_i, NADH) seem to be essentially constant in intact heart in vivo at different workloads/beating frequencies [1,2,15]. In agreement with the experimental studies [1,2,15,18–27], our model predicts the following metabolite

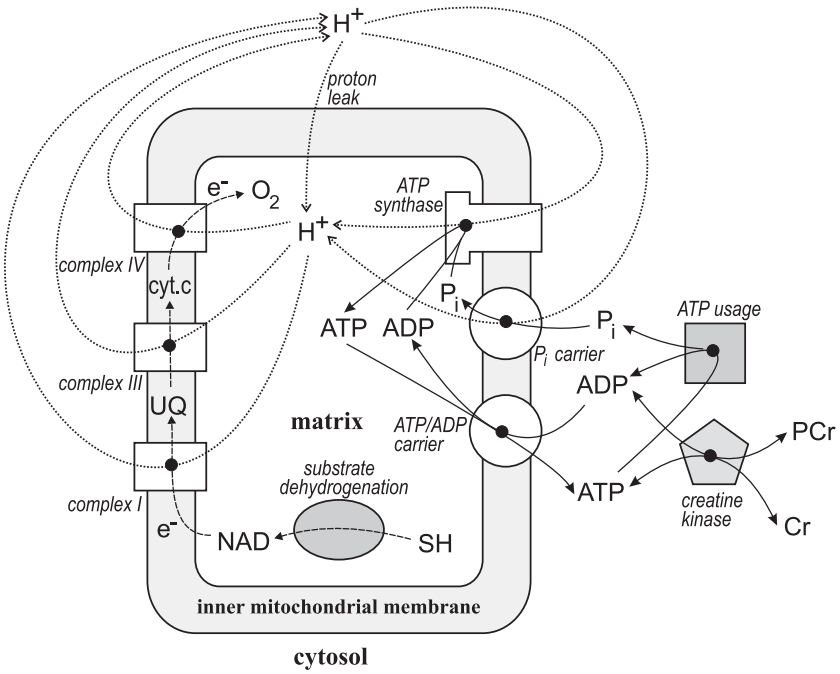

Fig. 1. General scheme of the oxidative phosphorylation system. The enzymes/processes/metabolic blocks taken into account explicitly within the computer model of the oxidative phosphorylation system are depicted. SH, respiratory substrate; UQ, ubiquinone; cyt.c, cytochrome *c*.

concentrations for the lowest work intensity: free $[ADP]_e$=31.7 μM, ATP/ADP=210 ($[ATP]_e$=6.67 mM), $[PCr]_e$=12.2 mM (PCr/Cr=0.95), PCr/ATP=1.83, $NADH/NAD^+$=0.38. These changes as compared to skeletal muscle model were necessary because heart is never in the resting state under physiological conditions, and because VO_2 (scaled per mitochondria volume or per mg of mitochondrial protein) and $[ADP]_e$ at low work in heart are higher, while the PCr/Cr ratio is lower than in resting skeletal muscle. PCr/Cr is equal to about 1 in heart and about 3–4 in resting skeletal muscle.

Using the parameter values accepted in our model (increase in the respiration rate in relation to resting skeletal muscle due to the greater mitochondria volume, the lower PCr/Cr ratio (higher [ADP]) and the lower $[P_i]$ at a given [ADP] in heart) we obtain the value of the respiration rate at the lowest heart work equal to 2.55 mM/min, which is close to the minimal value of this parameter measured in dog heart. In our theoretical studies we generate VO_2 values from 2.55 mM/min (low work intensity) to 11.2 mM/min (high work intensity).

A broad range of VO_2 between about 1 mM/min and ≫20 mM/min is encountered in experimental studies at different work intensities in mammalian heart [1,18,21–25]. The values depend on experimental conditions and on the manner of heart stimulation. The VO_2 in heart depends also very significantly on the animal size—it is much greater in smaller animals than in larger animals. For rat the typical range is about 8–>20 mM/min [18,21,22,26], for rabbit it is 4.6–6.6 mM/min [15] and for dog it is about 2–10 mM/min [1,25]. The model used in the present article generates the range of VO_2 (determined by an appropriate range of ATP usage; see below) encountered in dog heart. The previously published model of oxidative phosphorylation in skeletal muscle [11], that constitutes the basis for the development of the model for heart, concerns medium-size mammals (dogs, humans and so on). This fact is beneficial for our purposes, since the best experimental data concerning metabolite concentrations and oxygen consumption in intact heart in vivo have been published for dog heart [1,2,25].

2.2. Computer simulations

The low-work steady-state in heart described above constituted the starting point for simulations concerning high-work steady-states. In these simulations the low-work energy demand (rate constant of ATP usage) was increased n times, where n was between 1 and 5 (highest work intensity analysed in the present study); in subsequent simulations n was equal to 1, 1.5, 2, 2.5, 3, 3.5, 4, 4.25, 4.5, 4.75 and 5. In different tested mechanisms of the regulation of oxidative phosphorylation a variable set of complexes in the ATP-producing block was directly activated by n or n^2 times. Generally, the n-fold activation of a given step meant that the new rate constant(s) of this step k' was (were) n times greater than the old rate constant(s) k:

$$k' = n*k \tag{1}$$

For instance, in the kinetic expressions for ATP usage:

$$v_{UT} = k_{UT}\frac{1}{1+\frac{K_{mA}}{ATP_{te}}} \tag{2}$$

for substrate dehydrogenation:

$$v_{DH} = k_{DH} \frac{1}{\left(1 + \frac{K_{mN}}{NAD^+/NADH}\right)^{p_D}} \quad (3)$$

and for cytochrome oxidase:

$$v_{C4} = k_{C4} a^{2+} c^{2+} \frac{1}{1 + \frac{K_{mO}}{O_2}}$$

the rate constants k_{UT}, k_{DH} and k_{C4}, respectively, were multiplied by n. It is worth to mention that the concentration of the reduced form of cytochrome a_3 [a^{2+}] appearing in the kinetic equation for cytochrome oxidase depends on the protonmotive force (see Appendix A), and thus the kinetics of cytochrome oxidase directly depends on this potential as well.

The complete description of the model of oxidative phosphorylation in intact heart is given in Appendix A and located on the web site http://awe.mol.uj.edu.pl/~benio.

3. Theoretical results

In case of the output-activation mechanism, no direct activation of any component of the ATP-producing block accompanied the direct stimulation of ATP usage. The relationship between VO_2 and selected metabolite concentrations ($[ADP]_e$, $[PCr]_e$, $[P_i]_e$, and mitochondrial NADH/NAD^+) simulated for the output-activation mechanism is presented in Fig. 2. It is clear that the increase in work intensity (the rate constant k_{UT} was increased) is accompanied by huge relative changes in metabolite concentrations. Furthermore, it should be noted that the elevation of VO_2 is self-limited in this case—the increase in k_{UT} causes a decrease in [ATP] to a very low level and this inhibits ATP usage (compare Eq. (2)), while in the case of the each-step-activation mechanism (see below) a potentially unlimited increase in VO_2 may take place.

A quite similar kinetic behaviour of the system, presented in Fig. 3, takes place in the case of the input/output activation mechanism where substrate dehydrogenation was activated (the rate constant k_{DH} was increased) to the same extent as ATP usage. Here, the NADH/NAD^+ ratio tends rather to increase than decrease (because NADH production is activated more than NADH consumption), but the concentrations of the remaining metabolites change to a large extent.

In order to check if a large direct activation of substrate dehydrogenation (much greater than the activation of ATP usage) is able to improve significantly the stability of metabolite concentrations (Fig. 4) substrate dehydrogenation was activated n^2 times in parallel with an n-fold activation of ATP usage. One can see that the changes in [ADP], [PCr] and [P_i] are still huge. Additionally, in this case the NADH/NAD^+ ratio increases very significantly, from 0.38 at low work intensity to 3.5 at high work intensity (because NADH production is activated much more than NADH consumption).

As it was discussed before, essentially no changes in [ADP], [PCr], [P_i] and NADH/NAD^+ take place during transition between different workloads in the intact heart in vivo. Theoretical results shown in Figs. 2–4 clearly indicate that both the output-activation mechanism and the input/output activation mechanism can not account for those experimental findings.

Fig. 5 presents the simulated relationship between VO_2 and [ADP], [PCr], [P_i] and NADH/NAD^+ in the case of the each-step-activation mechanism. The rate constants of substrate dehydrogenation and all steps of oxidative phosphorylation (but proton leak) were increased to the

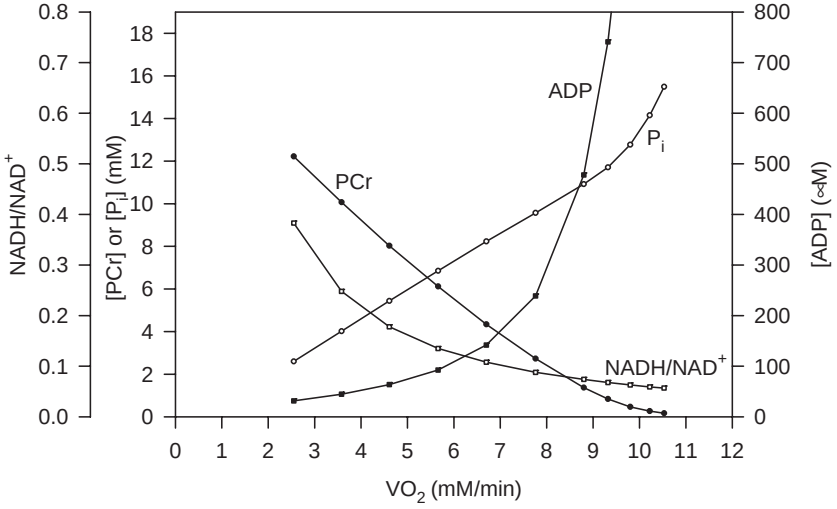

Fig. 2. Simulated relationship between VO_2 and cytosolic [ADP], [PCr], [P_i] and NADH/NAD^+ for the output-activation mechanism. Only ATP usage was directly activated during transition from low work intensity to higher work intensities. Oxidative phosphorylation was activated indirectly by an increase in [ADP].

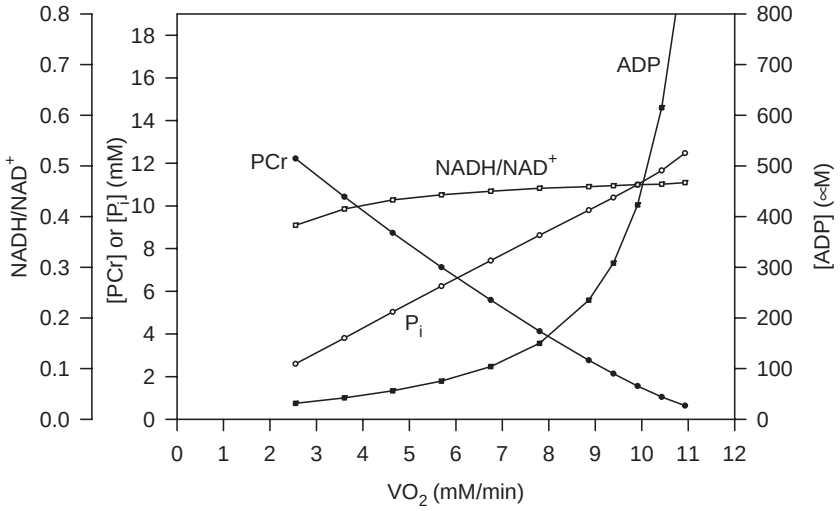

Fig. 3. Simulated relationship between VO_2 and cytosolic [ADP], [PCr], [P_i] and NADH/NAD^+ for the input/output-activation mechanism with moderate activation of substrate dehydrogenation. Only ATP usage and substrate dehydrogenation were directly activated by factor *n* during transition from low work intensity to higher work intensities. Oxidative phosphorylation was activated indirectly by an increase in [ADP] and [NADH].

same extent (*n* times) when the rate constant of ATP usage was multiplied by n. The proton leak was not activated because this would be equivalent to an elevated heat production and net energy waste. One can easily see that this each-step-activation mechanism gives an almost perfect stability of metabolite concentrations at different work intensities—the curves representing particular metabolite concentrations are almost horizontal. The small changes in metabolite concentrations are due to the fact that proton leak was not directly stimulated in these simulations. The kinetic behaviour of the system predicted by the each-step-activation mechanism agrees very well with the results of experimental studies obtained in intact heart in vivo.

Taken together, the computer simulations presented so far strongly suggest that the oxidative phosphorylation system in mitochondria as a whole must be directly activated in order to avoid significant changes in metabolite concentrations during transitions between different work intensities. However, the question remains whether all oxidative phosphorylation complexes have to be directly stimulated or it is enough to activate only some of them. In order to answer this question, a series of simulation sets were performed where all oxidative phosphorylation complexes but one, different in each set, were directly stimulated to the same extent as in the set of simulations presented in Fig. 5. The theoretical results concerning the set of simulations where all oxidative phosphorylation complexes but the ATP/ADP carrier were directly activated is presented in Fig. 6. One can see that switching off the direct activation of only this one complex causes significant changes in

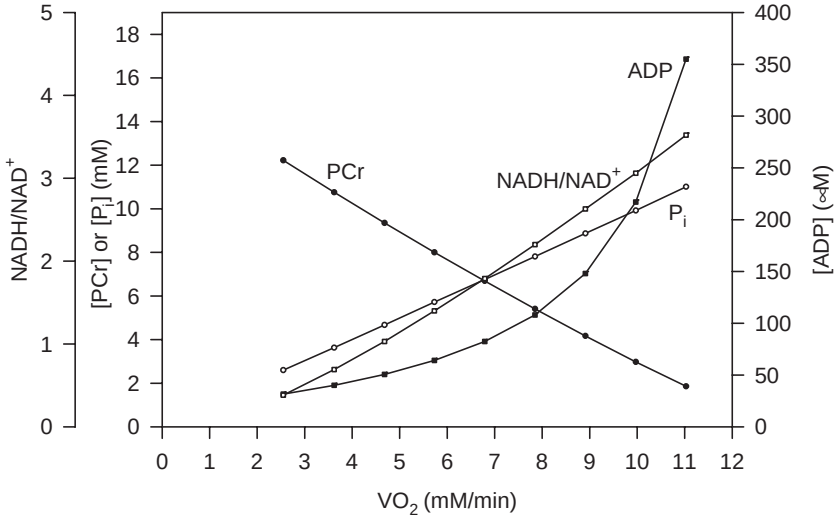

Fig. 4. Simulated relationship between VO_2 and cytosolic [ADP], [PCr], [P_i] and NADH/NAD^+ for the input/output-activation mechanism with strong activation of substrate dehydrogenation. Only ATP usage and substrate dehydrogenation were directly activated (by factor *n* and n^2, respectively) during transition from low work intensity to higher work intensities. Oxidative phosphorylation was activated indirectly by an increase in [ADP] and [NADH].

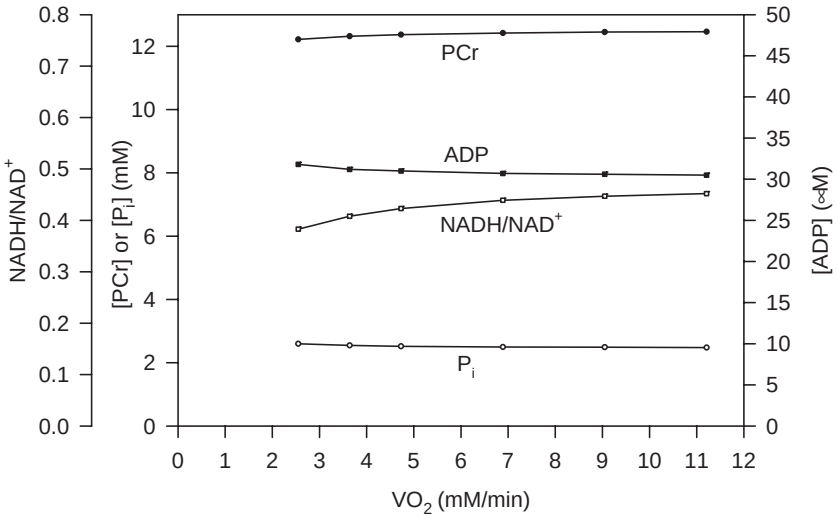

Fig. 5. Simulated relationship between VO_2 and cytosolic [ADP], [PCr], [P_i] and $NADH/NAD^+$ for the each-step-activation mechanism. ATP usage, substrate dehydrogenation and all steps of oxidative phosphorylation were directly activated to the same extent during transition from low work intensity to higher work intensities.

metabolite concentrations, although not so great as those seen in Figs. 2–4. Additionally, the lack of direct activation of the ATP/ADP carrier could not be compensated by an increased direct activation of other oxidative phosphorylation steps [theoretical results not shown]—ADP concentration was equal to at least 60 μM at high work intensity and the $NADH/NAD^+$ ratio increased dramatically when substrate dehydrogenation and other oxidative phosphorylation complexes were activated to a high extent.

We examined the effect of switching off activation of only one step for all other steps: complex I, complex III, complex IV, ATP synthase and phosphate carrier. All simulations failed to reproduce the constant metabolite concentrations over the analysed range of VO_2—it was not possible to avoid significant changes in both $NADH/NAD^+$ and ADP. The effect of a switching off the direct activation of two or more complexes was much stronger than additive.

Generally, the above simulations deliver a strong evidence that at least most oxidative phosphorylation complexes, and probably all of them are directly activated during transition from low work intensity to high work intensity in intact heart in vivo.

4. Discussion

The present theoretical study demonstrates that neither direct activation of only ATP usage (output-activation mechanism) nor direct activation of both ATP usage and

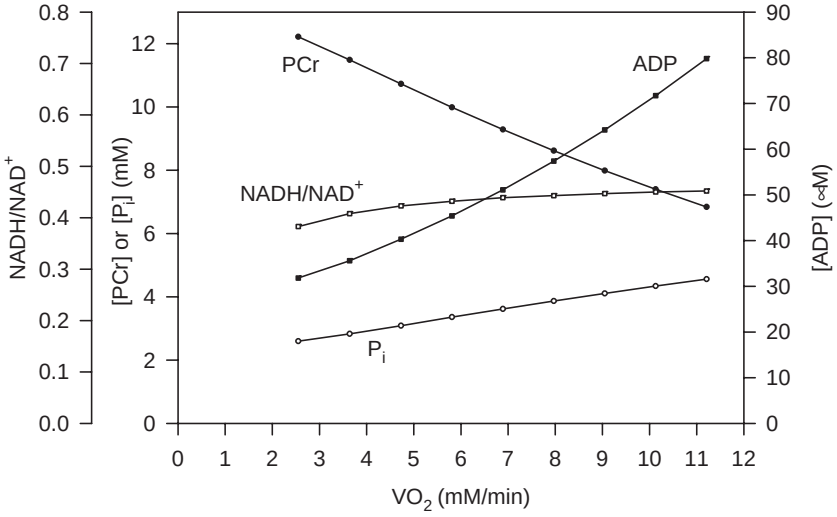

Fig. 6. Simulated relationship between VO_2 and cytosolic [ADP], [PCr], [P_i] and $NADH/NAD^+$ for the each-but-one-step-activation mechanism. ATP usage, substrate dehydrogenation and all steps of oxidative phosphorylation but ATP/ADP carrier were directly activated by the same factor during transition from low work intensity to higher work intensities.

substrate dehydrogenation (e.g. TCA cycle dehydrogenases and/or glycogen phosphatase) is able to reproduce the experimental finding of almost constant [ADP], [PCr], [P_i] and NADH/NAD^+ during transition between different work intensities in intact heart in vivo [1,2,15]. Only a direct activation by some intracellular factor/mechanism of probably all oxidative phosphorylation complexes and substrate dehydrogenation in parallel with the activation of ATP usage can account for the behaviour of the system in vivo.

In the present theoretical study a slightly modified version of the oxidative phosphorylation model [7,11] was used for intact heart. The theoretical predictions obtained in this study should be reliable, since this computer model has been tested for a broad set of different properties of the oxidative phosphorylation system [7,9–11,14,28]. The verification of the model concerns oxidative phosphorylation in isolated mitochondria, isolated hepatocytes and intact skeletal muscle. The correctly predicted system properties comprise, among others: (1) the values of fluxes (oxygen consumption, ATP turnover) and concentrations of metabolites (ADP, ATP, P_i, PCr, Cr, NADH/NAD^+ ratio, reduction level of cytochrome *c*, reduction level of cytochrome a_3, Δp—protonmotive force, O_2) in different steady-states imposed by various energy demands and oxygen concentrations; (2) changes over time of fluxes and metabolite concentrations during transitions between different steady-states (rest-to-work transition, aerobiosis-to-anaerobiosis transition); (3) the values of the flux control coefficients (defined within Metabolic Control Analysis (MCA) [29,30]) quantifying the control of particular enzymes/processes/metabolic blocks over the oxygen consumption flux in different steady-states (see below); (4) the dependence of the respiration rate on the activities/concentrations of different enzymes, obtained by titrating particular oxidative phosphorylation complexes with specific inhibitors. The last two properties are particularly important in the context of the present theoretical study because they are related to the kinetic properties of particular oxidative phosphorylation enzymes.

The need for a direct activation of all oxidative phosphorylation steps is also a direct consequence of the theoretical and experimental development of MCA [29–33]. In MCA, the flux control coefficient is defined as the ratio of a relative change in the overall flux through the system to a small relative change in enzyme activity/concentration, which is imposed on the system. The flux control coefficients of all enzymes in a given system sum up to unity. Experimental studies interpreted within the frame of MCA has demonstrated that the control over the oxygen consumption flux is more or less evenly distributed among different oxidative phosphorylation complexes. In particular, the flux control coefficient of the substrate dehydrogenation system over the oxygen consumption flux is quite small and equals about 0.1 in state 3 in isolated mitochondria respiring on pyruvate [31]. This implies that oxidative phosphorylation system cannot be activated significantly by activating only e.g. TCA cycle dehydrogenases causing an increase in the NADH/NAD^+ ratio. Furthermore, it should be noted that NADH/NAD^+ ratio changes little between steady-states with different work intensities in intact heart [15]. Therefore, the input/output activation mechanism cannot account for the discussed kinetic behaviour of the system. All oxidative phosphorylation complexes must be directly activated by some factor in order to allow a significant increase in this flux and at the same time to avoid changes in intermediate metabolite concentrations. In heart mitochondria, the metabolic control seems to be slightly differently distributed among particular enzymes than in skeletal muscle [32], but the values of flux control coefficients for particular complexes are also slightly different in different experimental studies concerning skeletal muscle mitochondria [31,32]. However, the most important property remains unchanged: flux control coefficients of all oxidative phosphorylation enzymes are of the same order of magnitude, at least in the isolated mitochondria system at saturating oxygen concentrations. The discussed property is also observed in saponine-skinned skeletal muscle fibres [34].

An idea similar to the each-step-activation mechanism, called ‘multisite modulation’, was proposed in a more general and abstract way by Fell and Thomas [35]. Kacser and Acerenza [36] proposed the ‘Universal Method’ for an increase in metabolic fluxes by biotechnological manipulation saying that when the control over the flux is distributed among all enzymes in a given system, the concentration/activity of all enzymes must be elevated in order to cause a large increase in the flux and low changes in intermediate metabolite concentrations.

Some other theoretical studies suggest different mechanisms underlying the regulation of oxidative phosphorylation in heart. Saks and co-workers [37,38] proposed that the constancy in [ADP] can be explained by the compartmentalized energy transfer. The authors assumed that the ATP consumption is very low in a slowly beating heart and therefore [P_i] is very low (a few μM), while [P_i] increases dramatically by 2–3 orders of magnitude during activation of heart work. This assumption stands in conflict with experimental studies where essentially no changes in [P_i] are reported in intact heart in vivo [1], and [P_i] is around 2–3 mM [18–20,22–24,26]. The authors incorporated the model of oxidative phosphorylation in mitochondria developed by Korzeniewski and co-authors to their model, but they assumed a relatively very low ATP usage (close to state 4 in isolated mitochondria), and then scaled it arbitrarily in order to cover the range of ATP usage in heart. As a result, their model works in fact in the range of the respiration and ATP usage shifted much to the left in Fig. 7A (see below) in relation to our model—in this range [P_i] is very low and just it, and not [ADP], is limiting for the respiration rate (this enables to generate large relative changes in VO_2 accompanied by only small relative changes in [ADP]—compare

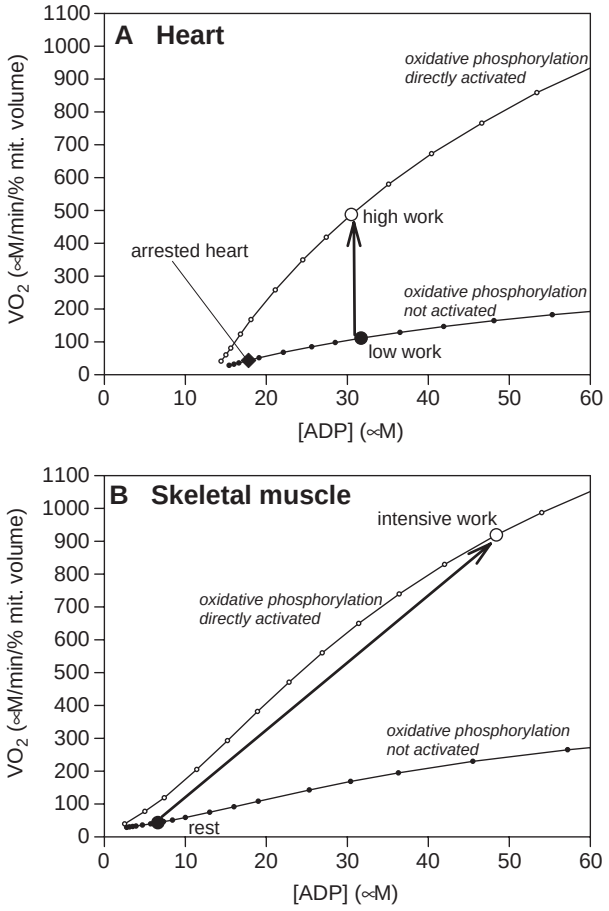

Fig. 7. Comparison of the regulation of oxidative phosphorylation in heart and in skeletal muscle. Respiration rate was scaled for relative mitochondria volume (% of the cell volume) in order to enable a direct comparison of these tissues. Phenomenological VO_2–[ADP] relationships (involving implicitly VO_2–[P_i] relationships) were simulated by changing the rate constant of ATP usage for not activated and for directly activated oxidative phosphorylation in heart and skeletal muscle. (A) In heart the low-work VO_2 and [ADP] are moderate, while during transition from low work to intensive work moderate relative increase in VO_2 is accompanied by no change in [ADP]. (B) In skeletal muscle the resting VO_2 and [ADP] are low, while during transition from rest to intensive work high relative increase in VO_2 is accompanied by moderate relative increase in [ADP]. Low and high work in heart correspond to the left and right points in Fig. 4 (VO_2 equal to 2.55 and 11.5 mM/min, respectively). Intensive work in skeletal muscle corresponds approximately to the maximal VO_2 during whole-body exercise (e.g. cycling). Details are given in the text.

Fig. 7A and the related discussion). Decrease in the NADH/NAD^+ ratio that must occur during low work→high work transition within the model developed by Saks and co-workers is also in contradiction with experimental results [15].

In isolated cardiac myocytes, NADH either increased or decreased during increased stimulation frequency, depending on the experimental system. Cortassa and co-workers [39] found a large increase in the NADH/NAD^+ ratio during an increase in work intensity in isolated cardiac myocytes and suggested the involvement of TCA cycle dehydrogenases activated by Ca^{2+} using their integrated model of oxidative phosphorylation and TCA cycle. However, these experimental findings cannot be extended to the intact heart in vivo, where the NADH/NAD^+ ratio remains almost constant during an increase in work intensity. It should also be noted that the isolated cardiac myocyte system is not physiological in several respects. For instance, humoral factors may be lacking in the perfusion medium and the electrical stimulation frequency is usually much lower than the beating frequency in intact heart.

Nevertheless, the model developed by Cortassa and co-workers [39] has potential advantages in relation to our model. It calculates explicitly the electrical potential through the inner mitochondrial membrane from the ion movement, and not from changes in ΔpH, as our model does. It involves explicitly particular components of the TCA cycle, while our model treats the whole substrate dehydrogenation system (TCA cycle, glycolysis, fatty acid β-oxidation and so on) as a black-box system described by a single kinetic equation. The advantage of our model (at least of its oxidative phosphorylation part) is that it is much better tested by comparison with various experimental data. The detailed description of the substrate dehydrogenation system is not so important, as long as one is not interested what happens within this system, because the metabolic control of substrate dehydrogenation over the oxygen consumption flux is low ([31], see discussion above). In our opinion, these models may be combined in order to produce a model that inherits the benefits of both models.

As to the model developed by the Saks' group [38,40–42], its advantage is to take into account the internal compartmentalization of the cardiac myocyte. In our opinion, the diffusion gradients and the displacement of creatine kinase from thermodynamic equilibrium is to some extent overestimated in this model, because it is mostly based on experimental data coming from the skinned fibre system, where unphysiological diffusion gradients may be present due to the existence of an unstirred layer (a skinned fiber is quite a large piece of tissue), especially when creatine is absent from the system. These gradients may be much reduced in intact heart due to blood circulation and creatine shuttle, and therefore neglecting these gradients may be quite a good (although certainly not perfect) approximation. However, this model emphasizes the role of Cr diffusion in overcoming the intracellular barriers for ADP diffusion and therefore it should be considered as complementary to our model, adding some important aspect of the kinetic properties of the cardiac myocyte bioenergetics.

Summing up, although we think that our model is best suited for the kind of theoretical studies carried out in the present article, other models can be useful for better understanding of other aspects of the considered system, not covered by our model.

It has been postulated that parallel activation of oxidative phosphorylation complexes is able to explain the variety in the kinetic properties of oxidative phosphorylation in different skeletal muscles and various experimental con-

ditions—parallel activation seems to be more intensive in oxidative muscle, neurally stimulated muscle and muscle in vivo than in glycolytic muscle, electrically stimulated muscle and perfused muscle [14]. The same explanation seems to apply to heart muscle—the larger changes in [ADP], [PCr], [P_i] and NADH/NAD^+ in perfused heart [18,26] and in isolated cardiac myocytes [43] than in intact heart in vivo may be explained by a disturbed parallel activation in the former.

Our model contains a simplified, phenomenological description of the NADH production system (TCA cycle, glycolysis, fatty acid β-oxidation and so on). Therefore, it does not involve explicitly the details of e.g. TCA cycle dehydrogenase activation by Ca^{2+}. Nevertheless, it is able to show that in principle the activation of different elements of the system may keep the NADH/NAD^+ ratio nearly constant.

The physical nature of the cytosolic factor directly activating oxidative phosphorylation complexes seems to have much to do with Ca^{2+}. The parallel activation of Δp production and Δp consumption was directly demonstrated during stimulation of respiration by vasopressin (a hormone acting via Ca^{2+}) in hepatocytes [44]. It has also been demonstrated that Ca^{2+} activates both Δp production and Δp consumption in isolated heart mitochondria [45] and skeletal muscle mitochondria [46]. Some experimental studies suggest that at least ATP synthase is directly activated by Ca^{2+} in heart [47,48]. A large variety of cell functions, such as excitation and contraction coupling in the muscles, are mediated by an increase in the cellular Ca^{2+}. It has been postulated that Ca^{2+} oscillations generated by cells in response to external stimuli (hormones and neural signals) can be integrated over time by some protein that causes e.g. phosphorylation and thus activation of oxidative phosphorylation complexes [9,10]. It must be stressed that while Ca^{2+} entry into mitochondria is necessary for the activation of TCA cycle dehydrogenases, the membrane oxidative phosphorylation complexes may be equally well activated by cytosolic Ca^{2+}.

Other factors may also contribute to the activation of oxidative phosphorylation during transition from low work to high work. For instance, a decrease in the NO (nitric oxide) concentration, a competitive inhibitor of cytochrome oxidase, would unblock this enzyme and thus activate the flux through the system [49,50]. It has been also postulated that mitochondrial ATP inhibits cytochrome oxidase at high ATP/ADP ratios, and that this inhibition is turned off by Ca^{2+} [51].

Our computer simulations have been very recently validated by Sharma and co-workers [52] who observed that a dobutamine-induced stimulation of heart work causing a 3-fold increase in the respiration rate was associated with essentially no changes in the ATP/ADP ratio, NADH/NAD^+ ratio and acetyl-CoA/CoA ratio, suggesting that several parts of the system were directly activated during elevated heart work.

The present study offers a simple explanation of the differences between the kinetic behaviour of oxidative phosphorylation in skeletal muscle and in heart. The differences are presented schematically in Fig. 7. The respiration rate in Fig. 7 was scaled for the relative mitochondria volume by expressing as percent of the cytosol volume in order to enable a direct comparison between heart (Fig. 7A) and skeletal muscle (Fig. 7B). The phenomenological VO_2–[ADP] relationships (involving implicitly the VO_2–[P_i] relationships) were determined from the cardiac and skeletal muscle models for no activation and for high each-step activation of oxidative phosphorylation. The slope of VO_2–[ADP] relationship for no activation of oxidative phosphorylation (lower curves in Fig. 7A and B) is smaller and [ADP] at which VO_2 reaches its minimum is lower in the skeletal muscle than in heart because in skeletal muscle [P_i] at a given [ADP] is much higher than in heart. For example, when [ADP] equals about 30 μM, [P_i] is equal to about 2.5 mM in heart vs. about 12 mM in skeletal muscle. In particular, in heart at [ADP] of about 15 μM, [P_i] decreases to very low values of several μM and becomes limiting for oxidative phosphorylation (this is why VO_2 reaches its minimal value at higher [ADP] in this case). Therefore, at very low work intensities in heart VO_2 may change significantly without significant changes in [ADP]. Thus, the total phosphate pool, affecting [P_i] in different physiological states, has a significant impact on the kinetic properties of oxidative phosphorylation. The differences in the phenomenological VO_2–[ADP] relationship for high direct activation of oxidative phosphorylation in heart and in skeletal muscle (upper curves in Fig. 7A and B) are due to the differences in the relationship for no direct activation discussed before and to the fact that in heart oxidative phosphorylation was directly activated 5 times (high work) while in skeletal muscle it was activated only 4 times (intensive, submaximal work).

The arrows in Fig. 7 indicate the transition from rest to intensive work in skeletal muscle and from low work to high work in heart. The low and high works in heart correspond to the lowest and highest VO_2 presented in Fig. 5, respectively. The intensive exercise in skeletal muscle corresponds to the maximal VO_2 during prolonged whole-body exercise (e.g. cycling) involving large muscle groups, in which mostly oxidative ATP production takes place (compare e.g. [14]). VO_2 increases over 20 times during transition from rest to intensive exercise; this is due to the 4-fold direct activation of oxidative phosphorylation and to the indirect activation of this process by an increase in [ADP] and [P_i]. The most important difference between heart and skeletal muscle seen in Fig. 7 is that in heart the maximal relative increase in VO_2 is moderate, and a perfect homeostasis of [ADP] is maintained during transition from low work to high work, while in skeletal muscle the maximal relative increase in VO_2 is much greater, but it is accompanied by a quite significant

increase in [ADP]. This difference is a direct consequence of the fact that in skeletal muscle the activation of ATP usage is much greater than the activation of ATP production, while in heart these metabolic blocks are activated to exactly the same extent.

The resting oxygen consumption in skeletal muscle equals about 0.3 mM/min [11]. During the development of the model of oxidative phosphorylation in heart this value was changed due to the increase in the mitochondria volume as well as due to the decrease in the total phosphate pool and increase in ATP usage introduced in order to obtain experimental values of [ADP], [P_i] and PCr/Cr. The resultant VO_2 was equal to 2.55 mM/min. This value is close to, or even slightly higher than the value of about 2 mM/min measured in intact dog heart in vivo at the lowest work intensity [1,25]. No additional increase in the activity of oxidative phosphorylation was necessary to reproduce this experimental value. This fact strongly suggests that there is, surprisingly, little or none direct activation of oxidative phosphorylation in slowly beating heart. This conclusion is supported by the fact that [ADP] in arrested heart is about half of that in beating heart [19], suggesting that changes in [ADP] and [P_i], and not the direct activation of oxidative phosphorylation are responsible for the transition from arrested heart to slowly beating heart. Therefore, the point indicating the low-work steady state in heart is situated on the line representing the VO_2–[ADP] relationship for no direct activation of oxidative phosphorylation.

Summing up, computer simulations performed using the model of oxidative phosphorylation in intact heart in vivo developed in the present article decidedly support the each-step-activation mechanism of the regulation of oxidative phosphorylation proposed previously for skeletal muscle. In intact heart in vivo, probably all oxidative phosphorylation complexes are directly activated by some mechanism involving Ca^{2+} in parallel with a direct activation of ATP usage and substrate dehydrogenation during transition from low-work steady-state to high-work steady-state. The regulation of oxidative phosphorylation in heart is much more homeostatic than in skeletal muscle because all elements of the bioenergetic system seem to be activated to essentially the same extent, which enables a perfect homeostasis of metabolite concentrations and thermodynamic forces ([ADP], [PCr], [P_i], NADH/NAD+, protonmotive force, redox potential span of the respiratory chain) to be achieved.

The mechanism by which all oxidative phosphorylation complexes are directly activated at high work intensities remains unknown. Therefore, the present study constitutes a trial of predicting in the theoretical way the existence of some new, still undiscovered phenomena. Such theoretical predictions are common in physics (for example theoretical predictions of the existence of new elementary particles); however, in biology they represent an essentially novel approach.

Acknowledgements

This work was supported by The Leading Project for Biosimulation of the Ministry of Education, Culture, Sports, Science and Technology of Japan.

Appendix A

Concise complete kinetic description of the dynamic model of oxidative phosphorylation in intact heart. Subscripts: e, external (cytosolic); i, internal (mitochondrial); t, total; f, free; m, magnesium complex; j, monovalent.

Appendix A.1. Kinetic equations

(All reaction rates are expressed in μM min^{-1}).

Substrate dehydrogenation:

$$v_{DH} = k_{DH}\frac{1}{\left(1+\frac{K_{mN}}{NAD^+/NADH}\right)^{p_D}}$$

k_{DH}=96,293 μM min^{-1}, K_{mN}=100, p_D=0.8.

Complex I:

$$v_{C1} = k_{C1}\Delta G_{C1}$$

k_{C1}=819.61 μM mV^{-1} min^{-1}.

Complex III:

$$v_{C3} = k_{C3}\Delta G_{C3}$$

k_{C3}=467.90 μM mV^{-1} min^{-1}.

Complex IV:

$$v_{C4} = k_{C4}a^{2+}c^{2+}\frac{1}{1+\frac{K_{mO}}{O_2}}$$

k_{C4}=12.348 μM^{-1} min^{-1}, K_{mO}=120 μM (the apparent, phenomenological Michaelis constant for the whole oxidative phosphorylation system is equal to about 0.8 μM).

ATP synthase:

$$v_{SN} = k_{SN}\frac{\gamma-1}{\gamma+1}$$

k_{SN}=117706 μM min^{-1}, $\gamma = 10^{\Delta G_{SN}/Z}$.

ATP/ADP carrier:

$$v_{EX} = k_{EX}\left(\frac{ADP_{fe}}{ADP_{fe}+ATP_{fe}\times 10^{-\Psi_e/Z}} - \frac{ADP_{fi}}{ADP_{fi}+ATP_{fi}\times 10^{-\Psi_i/Z}}\right)\left(\frac{1}{1+K_{mADP}/ADP_{fe}}\right)$$

k_{EX}=187,185 μM min^{-1}, K_{mADP}=3.5 μM.

Phosphate carrier:

$$v_{PI} = k_{Pi}\left(Pi_{je}H_e - Pi_{ji}H_i\right)$$

k_{PI}=238.11 μM^{-1} min^{-1}.

ATP usage:

$$v_{UT} = k_{UT}\frac{1}{1+\frac{K_{mA}}{ATP_{te}}}$$

k_{UT}=12,244 μM min^{-1} (low work)−61,220 μM min^{-1} (high work), K_{mA}=150 μM.

Proton leak:

$$v_{LK} = k_{LK1}\left(e^{k_{LK2}\Delta p} - 1\right)$$

k_{LK1}=8.5758 μM min^{-1}, k_{LK2}=0.038 mV^{-1}.

Adenylate kinase:

$$v_{AK} = k_{fAK}ADP_{fe}ADP_{me} - k_{bAK}ATP_{me}AMP_e$$

k_{fAK}=862.10 μM^{-1} min^{-1}, k_{bAK}=22.747 μM^{-1} min^{-1}.

Creatine kinase:

$$v_{CK} = k_{fCK}ADP_{te}PCrH_e^+ - k_{bCK}ATP_{te}Cr$$

k_{fCK}=1.9258 μM^{-2} min^{-1}, k_{bCK}=0.00087538 μM^{-1} min^{-1}.

Appendix A.2. Set of differential equations

$$\dot{NADH} = (v_{DH} - v_{C1})R_{cm}/B_N$$

$$\dot{UQH}_2 = (v_{C1} - v_{C3})R_{cm}$$

$$\dot{c^{2+}} = (v_{C3} - 2v_{C4})2R_{cm}$$

$\dot{O}_2 = 0$ (constant saturated oxygen concentration $= 240\ \mu M$) or $\dot{O}_2 = -v_{C4}$

$$\dot{H}_i + = -(2(2+2u)v_{C4} + (4-2u)v_{C3} + 4v_{C1} - n_A v_{SN} - uv_{EX} - (1-u)v_{PI} - v_{LK})R_{cm}/r_{buffi}$$

$$\dot{ATP}_{ti} = (v_{SN} - v_{EX})R_{cm}$$

$$\dot{Pi}_{ti} = (v_{PI} - v_{SN})R_{cm}$$

$$\dot{ATP}_{te} = v_{EX} - v_{UT} + v_{AK} + v_{CK}$$

$$\dot{ADP}_{te} = v_{UT} - v_{EX} - 2v_{AK} - v_{CK}$$

$$\dot{Pi}_{te} = v_{UT} - v_{PI}$$

$$\dot{PCr} = -v_{CK}$$

R_{cm}=3.35 (cell volume/mitochondria volume ratio).

B_N=5 (buffering capacity coefficient for NAD).

Appendix A.3. Calculations

$$c^{3+} = c_t - c^{2+}$$

c_t=270 μM (=c^{2+}+c^{3+}, total concentration of cytochrome *c*).

$$UQ = U_t - UQH_2$$

U_t=1350 μM (=UQH_2+UQ, total concentration of ubiquinone).

$$NAD^+ = N_t - NADH$$

N_t=2970 μM (=NADH+NAD^+, total concentration of NAD).

$$AMP_e = A_{eSUM} - ATP_{te} - ADP_{te}$$

A_{eSUM}=6700.2 μM (=ATP_{te}+ADP_{te}+AMP_e, total external adenine nucleotide concentration).

$$ADP_{ti} = A_{iSUM} - ATP_{ti}$$

A_{iSUM}=16,260 μM (=ATP_{ti}+ADP_{ti}, total internal adenine nucleotide concentration).

$$Cr = C_{SUM} - PCr$$

C_{SUM}=25,000 μM (=Cr+PCr, total creatine concentration).

$$P_{SUM} = 45,582\ \mu M(= PCr + 3ATP_{te} + 2ADP_{te} + AMP_e + Pi_{te} + (3ATP_{ti} + 2ADP_{ti} + Pi_{ti})/R_{cm},$$

total phosphate pool)

Mg_{fe}=4000 μM (free external magnesium concentration).

$$ATP_{fe} = ATP_{te}/(1 + Mg_{fe}/k_{DTe})$$

k_{DTe}=24 μM (magnesium dissociation constant for external ADP).

$$ATP_{me} = ATP_{te} - ATP_{fe}$$

$$ADP_{fe} = ADP_{te}/(1 + Mg_{fe}/k_{DDe})$$

k_{DDe}=347 μM (magnesium dissociation constant for external ATP).

$$ADP_{me} = ADP_{te} - ADP_{fe}$$

Mg_{fi}=380 μM (free internal magnesium concentration).

$$ATP_{fi} = ATP_{ti}/(1 + Mg_{fi}/k_{DTi})$$

k_{DTi}=17 μM (magnesium dissociation constant for internal ATP).

$$ATP_{mi} = ATP_{ti} - ATP_{fi}$$

$$ADP_{fi} = ADP_{ti}/(1 + Mg_{fi}/k_{DDi})$$

k_{DDi}=282 μM (magnesium dissociation constant for internal ADP).

$$ADP_{mi} = ADP_{ti} - ADP_{fi}$$

T=298
R=0.0083 kJ mol^{-1} K^{-1}
F=0.0965 kJ mol^{-1} mV^{-1}
S=2.303 R T
Z=2.303 R T/F
u=0.861 (=$\Delta\Psi/\Delta p$)
pH_e=7.0 (=constant)

$$pH_i = -\log(H_i/1,000,000) \quad (H_i \text{ expressed in } \mu M)$$

$$\Delta pH = Z(pH_i - pH_e)$$

$$\Delta p = 1/(1-u)\ \Delta pH$$

$$\Delta\Psi = -(\Delta p - \Delta pH)$$

$$\Psi i = 0.65\Delta\Psi$$

$$\Psi e = -0.35\Delta\Psi$$

$$c_{0i} = \left(10^{-pHi} - 10^{-pHi-dpH}\right)/dpH$$
('natural' buffering capacity for H^+ in matrix)

dpH=0.001.

$$r_{buffi} = c_{buffi}/c_{0i}$$
(buffering capacity coefficient for H^+ in matrix)

c_{buffi}=0.022 M H^+/pH unit (buffering capacity for H^+ in matrix).

$$c_{0e} = \left(10^{-pHe} - 10^{-pHe-dpH}\right)/dpH$$
(natural buffering capacity for H^+ in cytosol)

dpH=0.001.

$$Pi_{je} = Pi_{te}/\left(1 + 10^{pHe-pK_a}\right)$$

$$Pi_{ji} = Pi_{ti}/\left(1 + 10^{pHi-pK_a}\right)$$

pK_a=6.8

$$\Delta G_{SN} = n_{A*}\Delta p - \Delta G_P$$
(thermodynamic span of ATP synthase)

$$\Delta G_P = \Delta G_{P0}/F + Z^*\log(1,000,000ATP_{ti}/(ADP_{ti}{*}Pi_{ti}))$$
(concentrations expressed in μM)

n_A=2.5 (phenomenological H^+/ATP stoichiometry of ATP syntahse).

ΔG_{P0}=31.9 kJ mol^{-1}.

$$E_{mN} = E_{mN0} + Z/2\log(NAD^+/NADH)$$
(NAD redox potential)

E_{mN0}=−320 mV.

$$E_{mU} = E_{mU0} + Z/2\log(UQ/UQH_2)$$
(ubiquinone redox potential)

E_{mU0}=85 mV.

$$E_{mc} = E_{mc0} + Z\log\left(c^{3+}/c^{2+}\right)$$
(cytochrome c redox potential)

E_{mc0}=250 mV.

$$E_{ma} = E_{mc} + \Delta p(2+2u)/2$$
(cytochrome a_3 redox potential)

$$A_{3/2} = 10^{(E_{ma}-E_{ma0})/Z}\left(a^{3+}/a^{2+}\text{ ratio}\right)$$

$$a^{2+} = a_t/\left(1 + A_{3/2}\right)$$
(concentration of reduced cytochrome a_3)

$$a^{3+} = a_t - a^{2+}$$

a_t = 135 μM

E_{ma0}=540 mV.

$$\Delta G_{C1} = E_{mU} - E_{mN} - \Delta p4/2$$
(thermodynamic span of complex I)

$$\Delta G_{C3} = E_{mc} - E_{mU} - \Delta p(4-2u)/2$$
(thermodynamic span of complex III)

References

[1] L.A. Katz, J.A. Swain, M.A. Portman, R.S. Balaban, Relation between phosphate metabolites and oxygen consumption of heart in vivo, Am. J. Physiol. 256 (1989) H265–H274.
[2] R.S. Balaban, H.L. Kantor, L.A. Katz, R.W. Briggs, Relation between work and phosphate metabolite in the in vivo paced mammalian heart, Science 232 (1986) 1121–1123.
[3] B. Chance, G.R. Williams, The respiratory chain and oxidative phosphorylation, Adv. Enzymol. 17 (1956) 65–134.
[4] J.A. Jeneson, R.W. Wiseman, H.V. Westerhoff, M.J. Kushmerick, The signal transduction function of oxidative phosphorylation is at least second order in ADP, J. Biol. Chem. 271 (1996) 27995–27998.
[5] J.G. McCormack, A.P. Halestrap, R.M. Denton, Role of calcium ions in regulation of mammalian intramitochondrial metabolism, Physiol. Rev. 70 (1990) 391–425.
[6] R.G. Hansford, Control of mitochondrial substrate oxidation, Curr. Top. Bioenerg. 10 (1980) 217–277.
[7] B. Korzeniewski, J.-P. Mazat, Theoretical studies on the control of oxidative phosphorylation in muscle mitochondria: application to mitochondrial deficiencies, Biochem. J. 319 (1996) 143–148.
[8] B. Korzeniewski, Regulation of ATP supply during muscle contraction: theoretical studies, Biochem. J. 330 (1998) 1189–1195.

[9] B. Korzeniewski, Regulation of ATP supply in mammalian skeletal muscle during resting state→intensive work transition, Biophys. Chemist. 83 (2000) 19–34.
[10] B. Korzeniewski, Theoretical studies on the regulation of oxidative phosphorylation in intact tissues, Biochim. Biophys. Acta 1504 (2001) 31–45.
[11] B. Korzeniewski, J.A. Zoladz, A model of oxidative phosphorylation in mammalian skeletal muscle, Biophys. Chemist. 92 (2001) 17–34.
[12] M. Tonkonogi, K. Sahlin, Rate of oxidative phosphorylation in isolated mitochondria from human skeletal muscle: effect of training status, Acta Physiol. Scand. 161 (1997) 345–353.
[13] B. Korzeniewski, J.A. Zoladz, Training-induced adaptation of oxidative phosphorylation in skeletal muscle, Biochem. J. 374 (2003) 37–40.
[14] B. Korzeniewski, Regulation of oxidative phosphorylation in different muscles and various experimental conditions, Biochem. J. 375 (2003) 799–804.
[15] F.W. Heineman, R.S. Balaban, Effects of afterload and heart rate on NAD(P)H redox state in the isolated rabbit heart, Am. J. Physiol. 264 (1993) H433–H440.
[16] J. Schaper, E. Meiser, G. Stammler, Ultrastructural morphometric analysis of myocardium from dogs, rats, hamsters, mice, and from human hearts, Circ. Res. 56 (1985) 377–391.
[17] D.G. Allen, C.H. Orchard, Myocardial contractile function during ischemia and hypoxia, Circ. Res. 60 (1987) 153–168.
[18] A.H.L. From, S.D. Zimmer, S.P. Michurski, P. Mohanakrishnan, V.K. Ulstad, W.J. Thoma, K. Ugurbil, Regulation of the oxidative phosphorylation rate in the intact cell, Biochemistry 29 (1990) 3731–3743.
[19] R.A. Kauppinen, J.K. Hiltunen, I.E. Hassinen, Subcellular distribution of phosphagens in isolated perfused rat heart, FEBS Lett. 112 (1980) 273–276.
[20] Y. Kashiwaya, K. Sato, N. Tsuchiya, S. Thomas, D.A. Fell, R.L. Veech, J.V. Passonneau, Control of glucose utilization in working perfused rat heart, J. Biol. Chem. 269 (1994) 25502–25514.
[21] B. Wan, C. Doumen, J. Duszyński, G. Salama, T.C. Vary, K.F. LaNoue, Effects of cardiac work on electrical potential gradient across mitochondrial membrane in perfused hearts, Am. J. Physiol. 265 (1993) H453–H460.
[22] F.M. Jeffrey, C.R. Malloy, Respiratory control and substrate effects in the working rat heart, Biochem. J. 287 (1992) 117–123.
[23] R. Kauppinen, Proton electrochemical potential of the inner mitochondrial membrane in isolated perfused rat hearts, as measured by exogenous probes, Biochim. Biophys. Acta 725 (1983) 131–137.
[24] M.H.J. Eijgelshoven, J.H.G.M. van Beek, I. Mottet, M.G.J. Nederhoff, C.J.A. Vanechteld, N. Westerhof, Cardiac high-energy phosphates adapt faster than oxygen-consumption to changes in heart-rate, Circ. Res. 75 (1994) 751–759.
[25] F.W. Heineman, R.S. Balaban, Control of mitochondrial respiration in the heart in vivo, Annu. Rev. Physiol. 52 (1990) 523–542.
[26] A.H.L. From, S.D. Zimmer, S.P. Michurski, P. Mohanakrishnan, V.K. Ulstad, W.J. Thoma, K. Ugurbil, Regulation of the oxidative phosphorylation rate in the intact cell, Biochemistry 29 (1990) 3731–3743.
[27] D.A. Scott, L.W. Grotyohann, J.Y. Cheung, R.C. Scaduto Jr., Ratiometric methodology for NAD(P)H measurement in the perfused rat heart using surface fluorescence, Am. J. Physiol. 267 (1994) H636–H644.
[28] B. Korzeniewski, J.A. Zoladz, Factors determining the oxygen consumption rate (VO_2) on-kinetics in skeletal muscle, Biochem. J. 379 (2004) 703–710.
[29] H. Kacser, J.A. Burns, The control of flux, Rate Control of Biological Processes, Cambridge University Press, Cambridge, 1973, pp. 65–104.
[30] R. Heinrich, T.A. Rapoport, A linear steady-state treatment of enzymatic chains. General properties, control and effector strength, Eur. J. Biochem. 42 (1974) 89–95.
[31] T. Letellier, M. Malgat, J.-P. Mazat, Control of oxidative-phosphorylation in rat muscle mitochondria—implications for mitochondrial myopathies, Biochim. Biophys. Acta 1141 (1993) 58–63.
[32] R. Rossignol, T. Letellier, M. Malgat, C. Rocher, J.-P. Mazat, Tissue variation of the control of oxidative phosphorylation: implication for mitochondrial diseases, Biochem. J. 347 (2000) 45–53.
[33] C. Reder, Metabolic control theory: a structural approach, J. Theor. Biol. 135 (1988) 175–201.
[34] E. Wisniewski, F. Gellerich, W.S. Kunz, Distribution of flux control among the enzymes of mitochondrial oxidative phosphorylation in calcium-activated saponin-skinned rat musculus soleus fibers, Eur. J. Biochem. 230 (1995) 549–554.
[35] D.A. Fell, S. Thomas, Physiological control of metabolic flux: the requirement for multisite modulation, Biochem. J. 311 (1995) 35–39.
[36] H. Kacser, L. Acerenza, A universal method for achieving increases in metabolite production, Eur. J. Biochem. 216 (1993) 361–367.
[37] M.K. Aliev, V.A. Saks, Compartmentalized energy transfer in cardiomyocytes: use of mathematical modeling for analysis of in vivo regulation of respiration, Biophys. J. 73 (1997) 428–445.
[38] M. Vendelin, O. Kongas, V.A. Saks, Regulation of mitochondrial respiration in heart cells analyzed by reaction-diffusion model of energy transfer, Am. J. Physiol. 278 (2000) C747–C764.
[39] S. Cortassa, M.A. Aon, E. Marban, R.L. Winslow, B. O'Rourke, An integrated model of cardiac energy metabolism and calcium dynamics, Biophys. J. 84 (2003) 2734–2755.
[40] V.A. Saks, A. Kuznetsov, T. Andrienko, Y. Usson, F. Appaix, K. Guerrero, T. Kaambre, P. Sikk, M. Lemba, M. Vendelin, Heterogeneity of ADP diffusion and regulation of respiration in cardiac cells, Biophys. J. 84 (2003) 3436–3456.
[41] M. Vendelin, M. Lemba, V.A. Saks, Analysis of functional coupling: mitochondrial creaatine kinase and adenine nucleotide translocase, Biophys. J. 87 (2004) 696–713.
[42] V.A. Saks, A.V. Kuznetsov, M. Vendelin, K. Guerrero, L. Kay, E.K. Seppet, Functional coupling as a basic mechanism of feedback regulation of cardiac energy metabolism, Mol. Cell. Biochem. 256/257 (2004) 185–199.
[43] R.L. White, B.A. Wittenberg, NADH fluorescence of isolated ventricular myocytes: effects of pacing, myoglobin and oxygen supply, Biophys. J. 65 (1993) 196–204.
[44] B. Korzeniewski, M.-E. Harper, M.D. Brand, Proportional activation coefficients during stimulation of oxidative phosphorylation by lactate and pyruvate or by vasopressin, Biochim. Biophys. Acta 1229 (1995) 315–322.
[45] V. Mildaziene, R. Baniene, Z. Nauciene, A. Marcinkeviciute, M. Morkuniene, V. Borutaite, B.N. Kholodenko, G.C. Brown, Ca^{2+} stimulates both the respiratory and phosphorylation subsystems in rat heart mitochondria, Biochem. J. 320 (1996) 329–334.
[46] N.I. Kavanagh, E.K. Ainscow, M.D. Brand, Calcium regulation of oxidative phosphorylation in rat skeletal muscle mitochondria, Biochim. Biophys. Acta 1457 (2000) 57–70.
[47] D.A. Harris, A.M. Das, Control of mitochondrial ATP synthesis by the heart, Biochem. J. 280 (1991) 561–573.
[48] P.R. Territo, V.K. Mootha, S.A. French, R.S. Balaban, Ca^{2+} activation of heart mitochondria oxidative phosphorylation: role of the F_0/F_1-ATPase, Am. J. Physiol. 278 (2000) C423–C435.
[49] C.E. Cooper, Nitric oxide and cytochrome oxidase: substrate, inhibitor or effector? TIBS 27 (2002) 33–39.
[50] G.C. Brown, Nitric oxide and mitochondrial respiration, Biochim. Biophys. Acta 1411 (1999) 351–369.
[51] I. Lee, E. Bender, B. Kadenbach, Control of mitochondrial membrane potential and ROS formation by reversible phosphorylation of cytochrome *c* oxidase, Mol. Cell. Biochem. 234/235 (2002) 63–70.
[52] N. Sharma, I.C. Okere, D.Z. Brunengraber, T.A. McElfresh, K.L. King, J.P. Sterk, H. Huang, M.P. Chandler, W.C. Stanley, Regulation of pyruvate dehydrogenase activity and citric acid cycle intermediates during high cardiac power generation, J. Physiol. 562 (2005) 593–603.